Appl. Phys. A 79, 2069–2073 (2004)
DOI: 10.1007/s00339-004-2864-y

Applied Physics A
Materials Science & Processing

W. GINDL[1,✉]
H.S. GUPTA[2]
T. SCHÖBERL[3]
H.C. LICHTENEGGER[4]
P. FRATZL[2]

Mechanical properties of spruce wood cell walls by nanoindentation

[1] BOKU Vienna, Department of Materials Science and Process Engineering, Gregor Mendel Strasse 33, 1180 Vienna, Austria
[2] Max Planck Institute of Colloids and Interfaces, Department of Biomaterials, 14424 Potsdam, Germany
[3] Erich Schmid Institute for Materials Science, Austrian Academy of Sciences, Jahnstrasse 12, 8700 Leoben, Austria
[4] Institute for Materials Science & Testing, Vienna University of Technology, Favoritenstrasse 9–11, 1040 Vienna, Austria

Received: 10 March 2004/Accepted: 26 March 2004
Published online: 10 June 2004 •

ABSTRACT In order to study the effects of structural variability, nanoindentation experiments were performed in Norway spruce cell walls with highly variable cellulose microfibril angle and lignin content. Contrary to hardness, which showed no statistically significant relationship with changing microfibril angle and lignin content, the elastic modulus of the secondary cell wall decreased significantly with increasing microfibril angle. While the elastic moduli of cell walls with large microfibril angle agreed well with published values, the elastic moduli of cell walls with small microfibril angle were clearly underestimated in nanoindentation measurements. Hardness measurements in the cell corner middle lamella allowed us to estimate the yield stress of the cell-wall matrix to be 0.34 ± 0.16 GPa. Since the hardness of the secondary cell wall was statistically not different from the hardness of the cell corner middle lamella, irrespective of high variability in cellulose microfibril angle, it is proposed that compressive yielding of wood-cell walls is a matrix-dominated process.

PACS 83.80.Mc

1 Introduction

With the increasing use of wood fibres as reinforcements in bio-based composites in recent years [1], the study of the mechanical properties of wood fibres and cell walls has become of great interest. One of the main issues is to understand the deformation behaviour of the wood-cell wall and its dependence on parameters such as structure and chemical composition. In softwoods like Norway spruce, the main structural elements, termed tracheids, are long hollow cells with a length of 2–4 mm, a diameter of 20–40 μm, and a wall thickness of 2–10 μm. The tracheid cell wall itself is of a composite structure, made up of up to 50% largely crystalline cellulose fibrils, which wind around the longitudinal cell axis in a characteristic spiral fashion. The tilt angle of the cellulose fibrils with respect to the longitudinal cell axis, often called the microfibril angle (MFA), can vary considerably within a single individual tree and is a key parameter in determining the mechanical strength and elasticity of wood [2, 3]. The cellulose fibrils are embedded in an amorphous matrix substance composed of roughly equal amounts of hemicellulose, a mixture of different polysaccharides, and lignin, a phenolic polymer [4]. Individual cells are bound together by the middle lamella, which consists predominantly of lignin [5].

Tensile tests on small tissue samples [3], individual fibres [6, 7], and cell-wall segments [8] with known MFA have provided an understanding of the effects of varying cell-wall structure on tensile properties. In-situ tensile tests in the X-ray beam allowed the establishment of a correlation between the deformation behaviour of wood tissue samples and MFA [9]. Finally, simultaneous stretching and infrared absorbance measurements (DMA-FTIR) on thin wood and paper foils revealed interactions between different wood cell wall polymers under mechanical loading [10].

Nanoindentation, a method of hardness testing at very small scale applied to the study of mechanical properties of a variety of materials [11–13], was introduced to the study of wood cell wall mechanics by Wimmer et al. [14] and Wimmer and Lucas [15]. The latter showed for wood that nanoindentation allows mechanical measurements at smaller scale than tensile tests, but found it not easy to interpret nanoindentation data, in particular elastic moduli, in view of discrepancies with tensile tests and model calculations.

In the present study, we perform nanoindentation experiments together with measurements of MFA and lignin content on a variety of Norway spruce cell walls, in order to elucidate the relationship between nanoindentation data and cell-wall structural variability.

2 Material and methods

2.1 *Determination of microfibril angle by small-angle X-ray scattering (SAXS)*

In order to investigate wood specimens representative of the whole spectrum of structural variability, Norway spruce (*Picea abies*) samples containing normal early and late wood, as well as compression wood and opposite wood, were selected. Compared to late wood, which is formed in summer, early wood of Norway spruce formed in spring consists of cells with wider diameters, thinner cell walls, and smaller cell lengths. Compression wood and opposite wood are tissues found on the compression and tension sides of

✉ Fax: +43-1/47654-4295, E-mail: wolfgang.gindl@boku.ac.at

leaning conifer stems and branches, respectively, the first being characterised by abnormally high microfibril angle and lignin content [16]. Prior to being prepared for nanoindentation and UV microscopy, the wood samples were characterised with SAXS to determine the MFA quantitatively. Cubes measuring about $1 \times 1 \times 1$ cm were taken from different wood tissues and 200-μm-thick tangential sections were cut with a microtome. The wood sections were mounted on a sample holder and inserted into a scanning SAXS instrument [17] equipped with a rotating Cu anode and a Bruker-AXS Hi-star detector. SAXS patterns were recorded in transmission with the longitudinal direction of the sample perpendicular to the incident beam (see sketch in Fig. 1). The MFA was determined quantitatively from the SAXS patterns as described in Lichtenegger et al. [18] and Reiterer et al. [19].

2.2 *Determination of cellular lignin content by UV microscopy*

According to Scott et al. [20], the concentration of lignin in the wood-cell wall can be determined with a UV microscope, making use of the proportionality between the lignin content and the absorbance at a wavelength of 280 nm. For this purpose, the thin wood foils used for SAXS were dehydrated in a graded series of ethanol (40%, 60%, 80%, and 100%) and acetone (100%) and embedded in epoxy resin [21]. Transverse sections with a constant thickness of 1 μm were cut from the cured epoxy block on a Leica ultramicrotome equipped with a diamond knife. The sections were placed on quartz-glass slides and covered with quartz cover slips. With a ZEISS MPM-800 photometer microscope, UV absorbance was determined in transmission mode in 20 secondary cell walls (S2) of each SAXS specimen, and in 41 cell corner middle lamellae (CCML). A measuring spot diameter of 0.5 μm allowed for an accurate placement in the middle of the S2 layer of the 2–5-μm-thick cell walls, and in the cell corners. The lignin content of the specimens was estimated using a coefficient of extinction of $15.6\,\mathrm{cm}^{-1}\,\mathrm{g}^{-1}$ proposed by Fergus et al. [5].

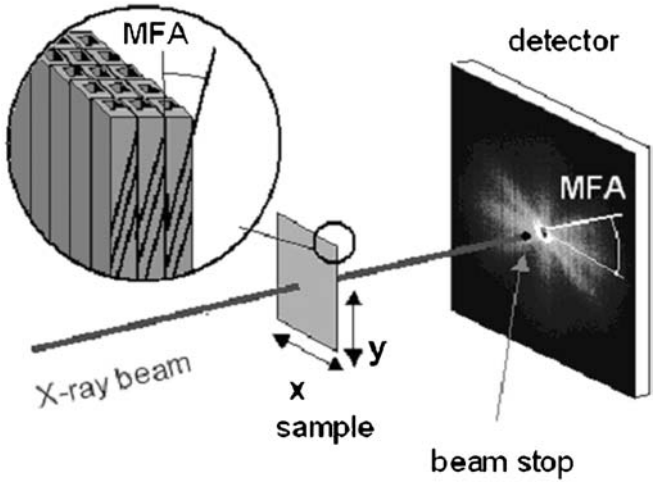

FIGURE 1 Measurement of MFA with SAXS: in the case of rectangular cells oriented perpendicular to the incident X-ray beam, the MFA can be directly read from the scattering pattern

2.3 *Measurement of cellular hardness and elastic modulus by nanoindentation*

The mechanical characterisation of the tracheid cell walls and cell corners measured with the UV microscope was carried out on a Dimension DI-3100 atomic force microscope (Digital Instruments, Veeco Metrology Group, Santa Barbara, CA) equipped with a Hysitron add-on force transducer for nanoindentation (Surface, Hueckelhoven, Germany). For this purpose, the dry samples embedded in epoxy resin, from which the sections for lignin determination had been cut, were mounted on metal plates clamped magnetically to the indenter sample stage. Quasi-static indentation tests were performed under environmental conditions in the same tissue region as measured in the UV microscope. In a force-controlled mode, the indenter tip (Berkovich-type triangular pyramid) was loaded to a peak force of 250 μN at a loading rate of 100 μN/s, held at constant load for 15 s, and unloaded at a rate of 100 μN/s. Figure 2 shows a light-microscope image of wood cells with indents after nanoindentation testing. From the load–depth curve recorded during a nanoindentation experiment (Fig. 3) the key parameters peak load ($P_{\max}$), depth at peak load (h), and initial slope of the unloading curve (S) are determined. According to the method developed by Oliver and Pharr [22], which is based on considerations by Doerner and Nix [23], the contact area A at $P_{\max}$ is determined and the hardness is obtained by dividing $P_{\max}$ by A. The analysis of the load–depth curve proceeds with the determination of the reduced elastic modulus E_r (1).

$$E_\mathrm{r} = \frac{1}{2}\sqrt{\pi}\,\frac{S}{\sqrt{A}}. \tag{1}$$

Here E_r is termed the reduced elastic modulus because it takes into account the compliance of the indenter tip by the relation

$$\frac{1}{E_\mathrm{r}} = \frac{1-\nu^2}{E} + \frac{1-\nu_0^2}{E_0}, \tag{2}$$

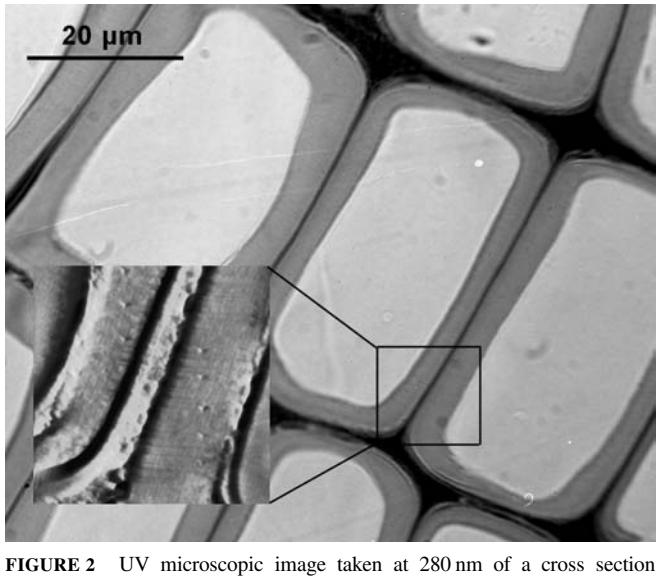

FIGURE 2 UV microscopic image taken at 280 nm of a cross section through Norway spruce cells. Grey values of the image correspond to lignin concentration. The *inset* shows an atomic force microscopy image of two cell walls and the middle lamella after indentation testing

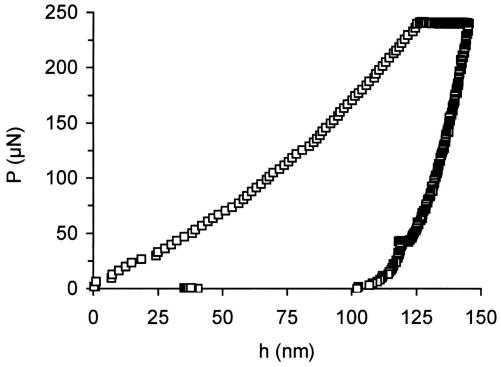

FIGURE 3 Load–depth curve of a nanoindentation test in a wood-cell wall

where E and ν are the elastic modulus and the Poisson ratio of the sample and E_0 and ν_0 stand for the same properties of the indenter tip. In soft materials like wood, the difference between E_r and E is negligibly small and no correction according to (2) was applied to our data.

3 Results

3.1 *Microfibril angle*

The results of the determination of cell-wall microfibril angle are shown in Table 1. A very high variability of mean MFA ranging from near 0° to 50° was obtained.

3.2 *Lignin content*

The average lignin content of the S2 cell-wall layers of five examined specimens and the average lignin content of the CCML is displayed in Fig. 4. All six groups of specimens showed a statistically significant difference in their average lignin concentration (ANOVA, $p < 0.05$). Regarding S2, the lowest lignin content was observed in LW_0 ($0.22\,g\,g^{-1}$), the maximum lignin concentration found in CW_50 ($40\,g\,g^{-1}$) being almost twice as high. Figure 4 shows a tendency of increasing lignin content with increasing MFA, resulting in a linear correlation coefficient of 0.93. The lignin content of the CCML did not vary significantly between the five examined specimens and is therefore presented as an overall average. CCML lignin content clearly surpasses the lignin content of S2.

3.3 *Hardness and elastic modulus*

Average hardness values determined by nanoindentation are shown in Fig. 5. Although a weak trend of decreasing hardness with increasing MFA in S2 is apparent from the box and whisker plot, no statistically significant difference (ANOVA, $p < 0.05$) was found between the hardness of all five studied S2 specimens. Furthermore, the average hardness of CCML is equal to the hardness of S2.

By contrast, the elastic modulus of S2 determined by nanoindentation shown in Fig. 6 shows a clear trend of decreasing stiffness with increasing MFA. At an MFA of 50° (CW_50), the elastic modulus is only half the modulus of sample LW_0, with near-0° MFA. The decrease of the elastic modulus with increasing MFA is not linear, but follows an s-shaped curve. The elastic modulus of CCML is similar to the elastic modulus of S2 specimens with large MFA (CW_50).

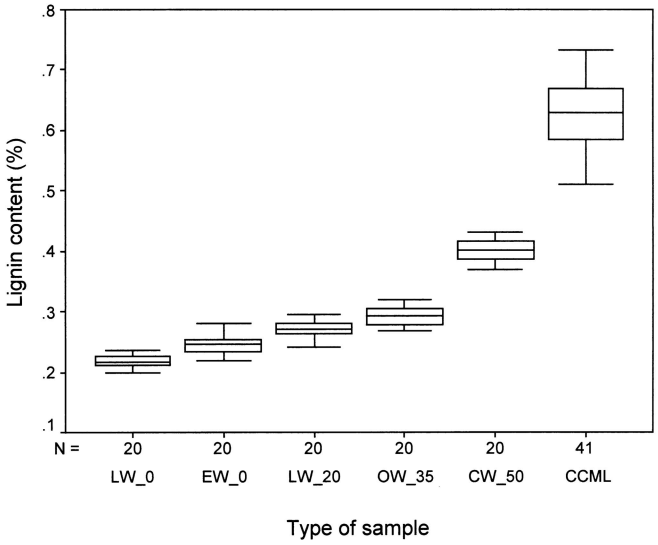

FIGURE 4 Lignin content of the S2 cell-wall layers of the five examined specimens, and average lignin content of CCML

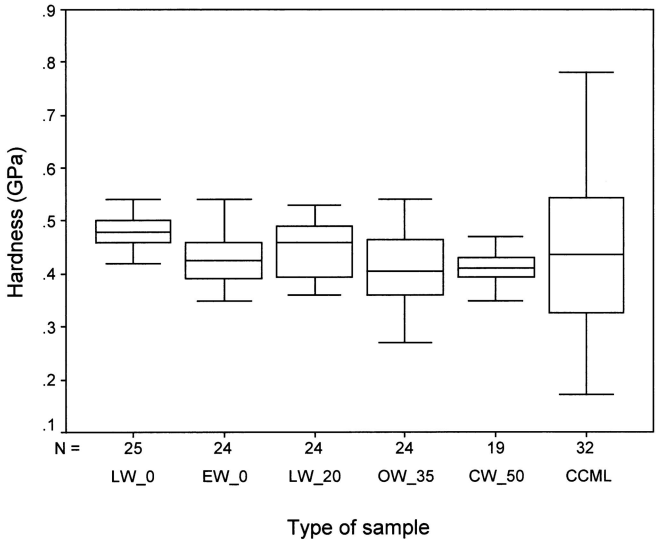

FIGURE 5 Hardness determined by nanoindentation

Sample description	Mean MFA (°)	Sample code
Normal early wood from a spruce stem	0	EW_0
Normal late wood from a spruce stem	0	LW_0
Normal late wood from a spruce stem	20	LW_20
Opposite wood from a spruce branch	35	OW_35
Compression wood from a spruce branch	50	CW_50

TABLE 1 Results of the determination of cell-wall microfibril angle by SAXS

4 Discussion

Samples selected for the present study represent the range of structural variability (i.e. lignin content and MFA) found in fibres of Norway spruce stems and branches [16]. Hardness values for five types of wood-cell

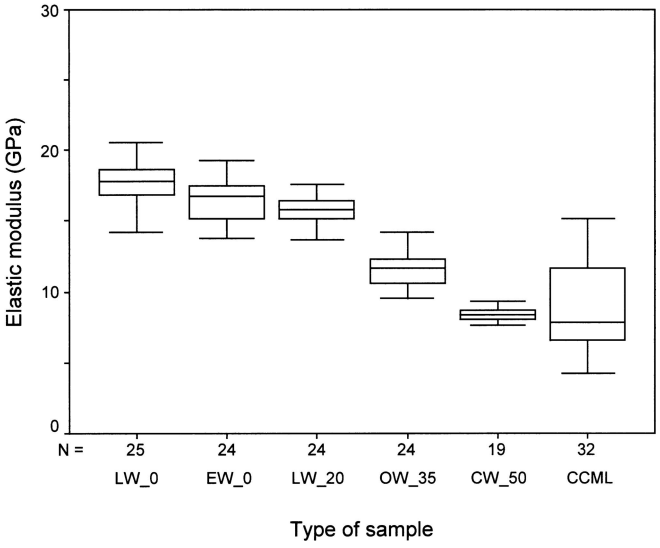

FIGURE 6 Elastic modulus determined by nanoindentation

walls with highly variable lignin content and MFA were very similar, and statistically not different from the hardness of the CCML (Fig. 5). While the hardness of a highly heterogeneous and mechanically anisotropic composite material such as the wood-cell wall is difficult to interpret in a straightforward manner, a closer inspection of the hardness of CCML, which is assumed to be mechanically isotropic and chemically less heterogeneous than S2, may help to understand the obtained results. Contrary to conventional hardness, which is determined from the area of the remaining imprint after unloading, nanoindentation hardness (H) is determined at peak load. This implies that not only plastic, but also elastic, deformation of the sample is considered. Therefore, the significance of nanoindentation hardness data depends on the ratio of elastic and plastic deformation, governed by the elastic modulus (E) and the yield stress (σ_y) of the material in question. For small E/σ_y, e.g. for polymers ($E/\sigma_y \approx 10$), the influence of the elastic pressure from the surrounding (elastically deformed) region on the extension of the plastic deformation zone becomes negligible, and σ_y is usually in the order of $2/3H$ [24].

In order to test the validity of the above estimates for wood (and thus the significance of our nanoindentation hardness values), consider the empirical relation in (3), derived by Larsson et al. [25] based on finite-element modelling and linking P_{max} (and thus H) to σ_y:

$$P_{max} = \frac{1.273}{(\tan 24.7)^2}\sigma_y \left(1+\frac{\sigma_r}{\sigma_y}\right)\left[1+\ln\left(\frac{E\tan 27.7}{3\,\sigma_y}\right)\right] h^2, \quad (3)$$

where σ_r is referred to as the reference stress and defined as the plastic stress level at a strain of 0.3 [25]. In a finite-element analysis of the plastic strain gradient under the indenter, Larsson et al. [25] assigned this strain to the zone immediately beneath the indenter tip. Giannakopoulos and Suresh [26] suggested a similar typical strain of 0.29 for the same zone. A ratio of 1.47 for σ_y/σ_r obtained in uniaxial compression tests on lignin-rich (45%), high-MFA (50°) compression wood of Norway spruce (Gindl 2003, unpublished) was chosen for the estimation of σ_y. Applying this value to the analysis of load–depth curves of nanoindentation experiments in 32 CCML samples with an average H of 0.47 ± 0.20 GPa, an average σ_y of 0.34 ± 0.16 GPa is obtained. In other words,

$$\sigma_y = 0.72\,H, \quad (4)$$

which agrees well with $\sigma_y \approx 2/3H$ proposed for polymers [24] and justifies the assumption of small E/σ_y in wood.

The similarity of hardness values measured for all S2 samples with the CCML hardness (Fig. 5) indicates that yielding of the wood-cell wall under nanoindentation load is a matrix-dominated phenomenon and largely independent of MFA. This agrees very well with results from axial compression tests on macro-sized specimens of Norway spruce, where the critical stress before failure of the cell wall due to kinking of cellulose microfibrils was independent of MFA [27].

Although hardness is apparently matrix-dominated, the percentage of lignin in the matrix shows no statistically significant effect on hardness variability in mature wood cells (Fig. 5). By contrast, in developing Norway spruce wood, significant changes of the hardness of the cell wall have been observed as a result of increasing lignification [28]. In a developing cell wall, cellulose fibrils coated with hemicellulose form an open network, whose empty spaces are progressively filled up with lignin [29–31]. As a natural consequence, the cell-wall density increases, explaining the overall increase in mechanical strength. In mature cell walls, as studied here, a change in lignin content does not change the overall cell-wall density [32]. A slight decrease of average S2 hardness with increasing lignin content is indicated in Fig. 5, but is not statistically significant.

Contrary to hardness data, changes in cell-wall structure and composition showed a clear effect on the elastic modulus of S2 (Fig. 6). With increasing MFA and increasing lignin content, the elastic modulus decreased in an s-shaped curve. Model calculations show that, due to low Young's modulus of lignin as compared to the cellulose fibrils, an increasing lignin concentration reduces the elastic modulus of the cell wall, but this effect was found to be minor compared to the strong influence of MFA [33, 34]. The average nanoindentation elastic modulus of 8.2 GPa for dry cell walls with an MFA of 50° agrees well with the value of 10 GPa measured in tensile tests on individual kraft pulp fibres of the same MFA [6]. An even better agreement is achieved with model calculations for native wood-cell walls, which yielded an elastic modulus of approximately 8 GPa at an MFA of 50° [34]. In contrast to samples with large MFA, the elastic modulus of cell walls with small MFA is clearly underestimated by nanoindentation, as already observed by Wimmer et al. [14]. The average nanoindentation elastic modulus of samples EW_0 and LW_0 of 17.1 GPa is considerably below values of 70 GPa measured by Page et al. [6] in tensile tests and 80 GPa calculated by Bergander and Salmén [34]. According to Swadener et al. [35], this discrepancy is due to the fact that the nanoindentation elastic modulus of an anisotropic material is a mixture of the moduli along all axes, which leads to an underestimation of the higher modulus. The extent of disagreement depends on the degree of anisotropy and the angle enclosed between the faces of the

indenter body and the load direction [36] and is more significant for small than for large MFA. Moreover, in a fibre composite loaded under compression along the fibre axis, the fibres (cellulose fibrils in the case of the wood-cell wall) are likely to buckle and, hence, not contribute as much to the stiffness as in tension. It is very likely, therefore, that the difference between the stiffness measured in tension and results from nanoindentation is at least partially related to the tension/compression asymmetry well known in fibre composites loaded along the fibre direction. Evidently, this effect will be much less important as soon as the MFA is sufficiently large. Considering all this, elastic moduli of wood-cell walls determined by nanoindentation have to be interpreted with caution.

In conclusion, our data indicate that the indentation hardness is essentially independent of the MFA, which suggests that it is governed by yield processes in the matrix. By contrast, the elastic modulus of the wood-cell wall is sensitive to the arrangement of the cellulose microfibrils. In the elastic regime the cellulose fibrils act as main load-bearing elements. Later on, as the deformation increases, the fibril–matrix interface may break and/or the matrix may yield such that the load transfer from matrix to fibers is affected.

ACKNOWLEDGEMENTS W.G. gratefully acknowledges financial support by the Austrian Science Fund FWF under Grant No. P15410-B03. H.C.L. was supported by the FWF under Grant No. T190-N02.

REFERENCES

1 A.K. Bledzki, J. Gassan: Prog. Polym. Sci. **24**, 221 (1999)
2 R.E. Mark: *Cell Wall Mechanics of Tracheids* (Yale University Press, New Haven 1967)
3 A. Reiterer, H. Lichtenegger, S. Tschegg, P. Fratzl: Philos. Mag. A **79**, 2173 (1999)
4 D. Fengel, G. Wegener: *Wood. Chemistry, Ultrastructure, Reactions* (De Gruyter, Berlin 1984)
5 B.J. Fergus, A.R. Procter, J.A.N. Scott, D.A.I. Goring: Wood Sci. Technol. **3**, 117 (1969)
6 D.H. Page, F. El-Hosseiny, K. Winkler, A.P.S. Lancaster: Tappi **60**, 114 (1977)
7 I. Burgert, K. Frühmann, J. Keckes, P. Fratzl, S.E. Stanzl-Tschegg: Holzforschung **57**, 661 (2003)
8 A. Bergander, L. Salmén: Holzforschung **54**, 654 (2000)
9 J. Keckes, I. Burgert, K. Frühmann, M. Müller, K. Kölln, M. Hamilton, M. Burghammer, S.V. Roth, S. Stanzl-Tschegg, P. Fratzl: Nat. Mater. **2**, 810 (2003)
10 M. Akerholm, L. Salmén: Polymer **42**, 963 (2001)
11 Z. Fan, J.G. Swadener, J.Y. Rho, M.E. Roy, G.M. Pharr: J. Orthopaed. Res. **20**, 806 (2002)
12 X. Li, B. Bhushan: Mater. Charact. **48**, 11 (2002)
13 H.C. Lichtenegger, T. Schöberl, M.H. Bartl, H. Waite, G.D. Stucky: Science **289**, 389 (2002)
14 R. Wimmer, B.N. Lucas, T.Y. Tsui, W.C. Oliver: Wood Sci. Technol. **31**, 131 (1997)
15 R. Wimmer, B.N. Lucas: IAWA J. **18**, 77 (1997)
16 T.E. Timell: *Compression Wood in Gymnosperms* (Springer, Berlin 1986)
17 P. Fratzl, H.F. Jakob, S. Rinnerthaler, P. Roschger, K. Klaushofer: J. Appl. Crystallogr. **30**, 765 (1997)
18 H. Lichtenegger, A. Reiterer, S.E. Stanzl-Tschegg, P. Fratzl: J. Struct. Biol. **128**, 257 (1999)
19 A. Reiterer, H.F. Jakob, S.E. Stanzl-Tschegg, P. Fratzl: Wood Sci. Technol. **32**, 5 (1998)
20 J.A.N. Scott, A.R. Procter, B.J. Fergus, D.A.I. Goring: Wood Sci. Technol. **3**, 73 (1969)
21 A.R. Spurr: Ultrastruct. Res. **26**, 31 (1969)
22 W.C. Oliver, G.M. Pharr: J. Mater. Res. **7**, 1564 (1992)
23 M.F. Doerner, W.D. Nix: J. Mater. Res. **1**, 601 (1986)
24 D. Tabor: 'Indentation Hardness and its Measurement: Some Cautionary Comments'. In: *Microindentation Techniques in Science and Engineering*, ed. by P.J. Blau, P.R. Lawn (American Society for Testing and Materials, Philadelphia 1986) pp. 129–159
25 P.L. Larsson, A.E. Giannakopoulos, E. Söderlund, D.J. Rowcliffe, R. Vestergaard: Int. J. Solids Struct. **33**, 221 (1996)
26 A.E. Giannakopoulos, S. Suresh: Scr. Mater. **40**, 1191 (1999)
27 W. Gindl, A. Teischinger: Composites Part A **33**, 1623 (2002)
28 W. Gindl, H.S. Gupta, C. Günwald: Can. J. Bot. **80**, 1029 (2002)
29 T. Fujino, T. Itoh: Holzforschung **52**, 111 (1998)
30 L.A. Donaldson, A.P. Singh: Holzforschung **52**, 449 (1998)
31 J. Hafrén, T. Fujino, T. Itoh: Plant Cell Physiol. **40**, 532 (1999)
32 R.M. Kellogg, C.B.R. Sastry, R.W. Wellwood: Wood Fiber Sci. **7**, 170 (1975)
33 L. Salmén, A. De Ruvo: Wood Fibre Sci. **17**, 336 (1985)
34 A. Bergander, L. Salmén: J. Mater. Sci. **37**, 151 (2002)
35 J.G. Swadener, J.Y. Rho, G.M. Pharr: J. Biomed. Mater. Res. **57**, 108 (2001)
36 W. Gindl, T. Schöberl: Composites Part A, in print, available online, DOI: 10.1016/j.compositesa.2004.04.002